Extreme Mechanics Letters 34 (2020) 100592

Contents lists available at ScienceDirect

Extreme Mechanics Letters

journal homepage: www.elsevier.com/locate/eml

Soft sensor for full dentition dynamic bite force

Sibo Cheng [a], Baohong Chen [b], Yuan Zhou [a], Minglong Xu [a], Zhigang Suo [b,*]

[a] State Key Lab for Strength and Vibration of Mechanical Structures, International Center for Applied Mechanics, School of Aerospace, Xi'an Jiaotong University, Xi'an 710049, PR China
[b] School of Engineering and Applied Sciences, Kavli Institute of Bionano Science and Technology, Harvard University, Cambridge, MA 02138, USA

ARTICLE INFO

Article history:
Received 1 August 2019
Received in revised form 17 September 2019
Accepted 16 October 2019
Available online 19 October 2019

Keywords:
Soft sensor
Bite force
Hydrogel
Dielectric elastomer

ABSTRACT

The measurement of bite force is important to dental care and research. Current sensors of bite force are made of hard materials, which do not conform to the irregular surfaces of teeth and constrain the movements of muscles. Here we propose a soft sensor made of a hydrogel and a dielectric elastomer. The sensor converts a mechanical force to a change in capacitance. We characterize the force under step loads at various speeds and under cyclic loads at different frequencies. We further use biocompatible materials and make arrayed sensors. The soft sensor easily conforms to the surfaces of individual teeth and captures dynamic bite forces in different regions of dentition. This work illustrates the potential of using soft sensors to collect massive data over irregular and dynamic surfaces of hard materials.

1. Introduction

In vertebrates, bite force is a trait that impacts whole-organism fitness [1]. Teeth are used not only to capture, subdue, and process preys, but also to compete for mates [2,3]. In the study of the feeding habits of various species, bite force is widely used to characterize masticatory systems, mechanical demands of diets, and dietary ecology [4]. Bite force has been measured for many species of animals, e.g., sharks [5], lizards [6], finches [7], and bats [8]. For humans, the maximum bite force (typically 600–800 N) is one indicator of the health of the masticatory system [9]. The bite force results from the action of the jaw elevator muscles [10]. The bite force has been widely used in dentistry to understand the mechanics of mastication, evaluate the therapeutic effects of prosthetic devices, and provide reference for the biomechanics of prosthetic devices [11,12]. Bite force is also used to evaluate masticatory function in patients before and after orthognathic surgery [13].

The sensing elements in existing bite force sensors are made of hard materials [14–21]. Biting a hard sensor, however, is different from biting a piece of food, especially a piece of soft tissue. The hard sensor is too stiff to deform, and does not conform to the irregular shapes of teeth. In addition, hard sensors affect the activity of elevator muscles, which results in poor reliability in recording the maximum voluntary bite force [22]. An improvement has been made to cover a sensor of a hard material with layers of a soft material [22], but it is desirable to design a sensor using soft materials.

Here we propose a soft sensor to measure the bite force. The soft sensor conforms to the rough surfaces of teeth, and captures full dentition dynamic bite force. The sensor is made of hydrogels and dielectric elastomers, and converts a bite force to a change in electric capacitance. We design a measurement system with high resolution to capture electrical signals. We characterize the signals of sensor under quasi-static and dynamic compressive loads using a jaw model. We further design an arrayed sensor to collect simultaneously the bite forces from different regions of dentition. It is hoped that the soft sensor will be further developed for clinical studies and for scientific studies of humans and other animals.

2. Experiments

Soft electronics and ionotronics are under intense development for applications in engineering and medicine [23–31]. This development has renewed the interest in evaluating soft materials, such as elastomers and hydrogels, in various tests, including fracture [32–34], fatigue [35–37], and adhesion [38–40]. The mechanical, electrical, and chemical characteristics of the soft materials have opened new fields of applications [41–53]. In particular, the combination of hydrogels and dielectric elastomers has enabled artificial muscles [54,55], artificial axons [56,57], and artificial skins [58–61]. For our sensors, hydrogels function as ionic conductors, and elastomers function as electrical insulators.

* Corresponding author.
E-mail addresses: mlxu@mail.xjtu.edu.cn (M. Xu), suo@seas.harvard.edu (Z. Suo).

https://doi.org/10.1016/j.eml.2019.100592
2352-4316/

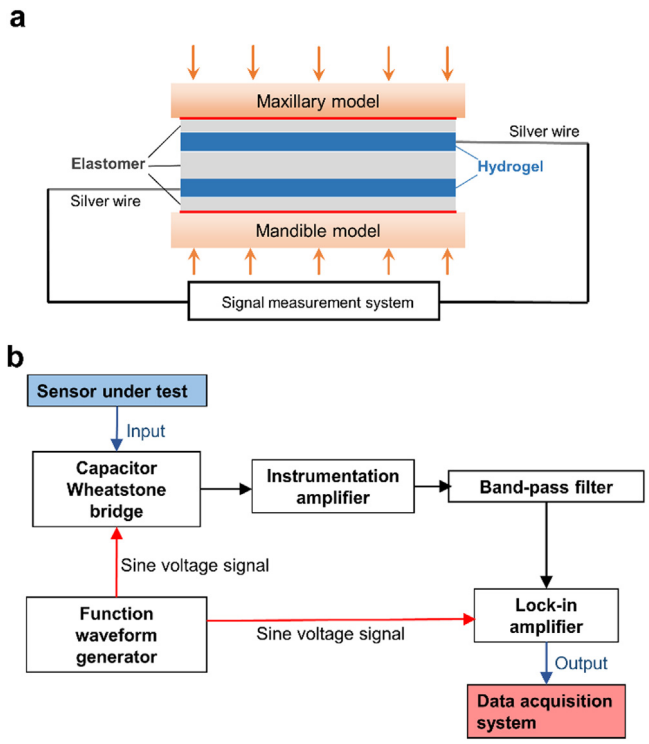

Fig. 1. Experimental setup. (a) The bite force sensor. (b) The measurement system . (For interpretation of the references to color in this figure legend, the reader is referred to the web version of this article.)

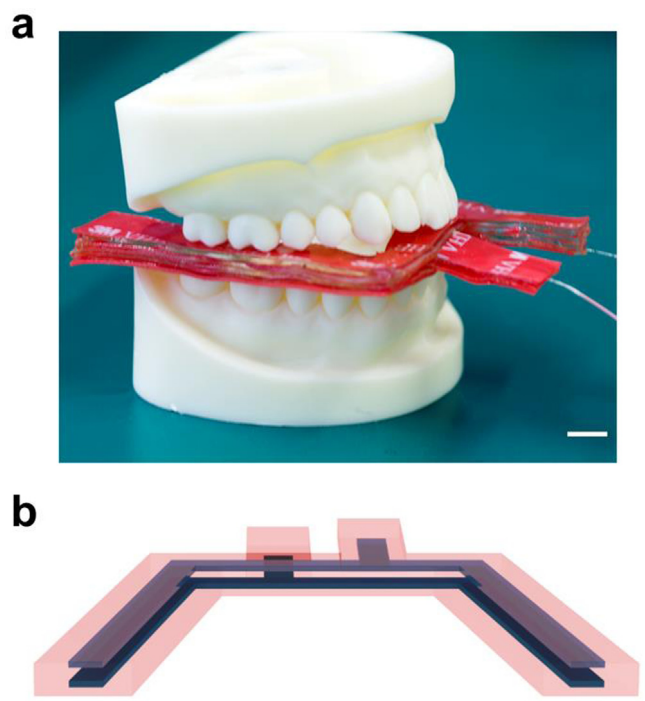

Fig. 2. (a) The sensor is sandwiched between model jaws. The soft sensor is covered by a thin polyethylene film (red color) to prevent external damage. Scale bar: 10 mm. (b) In a 3D model, the two blue layers are the hydrogels, and the extent parts in the front are used to connect with silver wires. The red translucent part in the diagram represents the elastomer layers . (For interpretation of the references to color in this figure legend, the reader is referred to the web version of this article.)

2.1. Experimental setup

We design a bite force sensor as a deformable capacitor (Fig. 1a). We put the sensor between the human maxillary and mandible models. The soft sensor is mainly made of two materials: a dielectric elastomers and a hydrogel. In our initial experiments, we use the acrylic elastomer (VHB^{TM}, 3M) as a soft dielectric, and the calcium-alginate–polyacrylamide (PAAm) hydrogel [34,62] as a soft ionic conductor. Both materials are tough. For example, the hydrogel has a flaw-insensitive size about 10 cm [36,53], much larger than the size of human tooth. The synthesis of the hydrogel is described in supporting information. We use the elastomer VHB^{TM} 4910 as the insulating layer between the ionic hydrogel conductors. The hydrogels are encapsulated in elastomeric layers to keep them from quickly drying out. The VHB elastomer is marketed as an adhesive tape, and comes with thin films of release layers of polyethylene (colored red) to avoid undesired adhesion. In the initial experiments, we leave the release layers on the top and bottom elastomers. Silver wires are used as interconnection between the ionic conductor and the measurement system. The whole structure is placed in the test machine (Zwick/Roell Z005) to deform under pressure. When the model jaws deform the soft sensor, the decrease of the thickness of insulating layer causes the capacitance of the sensor to increase. The change in capacitance is captured by the measurement system.

The initial capacitance of the sensor is estimated as $C = \varepsilon S/d$, where the permittivity of VHB^{TM} 4910 elastomer is $\varepsilon = 4.2 \times 10^{-11}$ F/m, the thickness of the elastomer is $d = 2 \times 10^{-3}$ m, and the area of the elastomer is $S = 7.9 \times 10^{-4}$ m^2, so that the capacitance is about 16.59 pF. The electric double layer (EDL) exists at the interfaces between the ionic conductor and metal electrodes, but negligibly affects the measured capacitance [24,58].

The measurement system consists of several parts (Fig. 1b). The Wheatstone bridge circuit improves the precision and reduces the interference from environments. The instrumentation amplifier enlarges the signals from the sensor. The high-pass Butterworth filter suppresses low-frequency noise. The functional waveform generator (DG4062, RIGOL) is used to output a test signal to bridge circuit, and a reference signal to lock-in amplifier (SR830, Stanford Research System). Both test and reference signals are sinusoidal of same frequency 1 kHz. The amplitude of the test signal is 2 V, and the reference signal of 4 V. The lock-in amplifier improves the signal-to-noise ratio (SNR) through signal difference calculation. Additionally, we use data acquisition system (QuantumX MX840B, HBM) for accessing high-frequency signals. Detailed circuit is in supporting information (Figure S3).

The photo of the sensor is shown in Fig. 2a. The model jaws are made of a hard material and simulate authentic dentition. A three-dimensional model of the sensor is shown in Fig. 2b. The upper and lower blue layers are hydrogels and extent parts in the front are used to connect with silver wires. Red translucent part in the diagram represents the elastomers. The photo of sensor after biting test is also shown in Figure S1. The bite marks can be clearly seen on the surface of the sensor.

2.2. Results and discussion

To relate the applied force and measured change in capacitance, we use a loading machine to homogeneously compress the sensor at different loading rates, and measure the changes in capacitance (Fig. 3a). We measure the capacitance of the sensor by using a LCR meter (HIOKI 3532-50 LCR HiTESTER). A sinusoidal signal is set at 1 V amplitude and 1000 Hz frequency. To characterize rate dependency of sensor, displacement rates

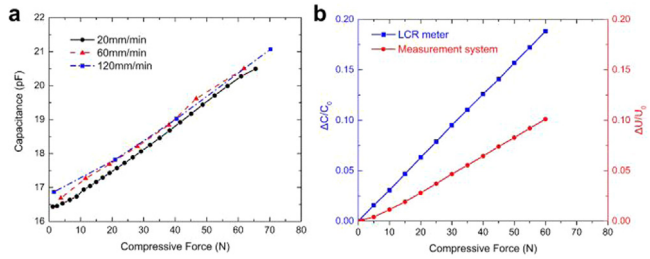

Fig. 3. Sensor characterization under homogeneous compression. (a) Compressive force is linearly related to capacitance. The sensor is compressed at 20, 60 and 120 mm/min. The displacement amplitude is 3 cm. (b) Changes of capacitance and voltage measured by LCR meter and bridge circuit, respectively. The loading rate is 10 mm/min and amplitude of 3 cm.

of 20, 60, and 120 mm/min are prescribed for compression. The maximum compressive displacement is 3 cm according to the chewing amplitude of humans [63]. The measured capacitance and applied compressive force are linearly related at all loading rates. The behavior of the sensor is nearly rate-independent.

The sampling frequency of LCR meters is usually low (∼1 Hz), limiting the measurement of capacitance in fast dynamic tests. However, our high-resolution bridge circuit (Fig. 1b) works at high sampling frequency (2.4 kHz), with output accuracy 0.01 millivolts, providing the potential to characterize the dynamic response of sensor at higher loading rates. The relationship between output voltage and applied force is also linear (Fig. 3b). To calibrate the sensor, we compare the capacitance by LCR meter and the voltage by bridge circuit. We linearly fit both curves, and obtain $\Delta U/U_0 = 0.00173F$, $\Delta C/C_0 = 0.00314F$. Accordingly, the relation between changes of voltage signal and capacitance is written as $\Delta U/U_0 = 0.551\Delta C/C_0$. Let $C_0 = \varepsilon \cdot S/D$, suppose the thickness of insulator after compression is $d = \lambda D$, where λ is less than 1. Due to the incompressibility, the changed electrode plates area is S/λ. Thus, the change of capacitance after deformation is $\Delta C = \varepsilon(S/D)\cdot(1/\lambda^2 - 1)$. For a measurement system with certain sensitivity, reducing the thickness of insulation layer can increase the change of capacitance and SNR.

To get the dynamic characteristics of the bite force sensor, we test the sensor under the step loading (Fig. 4). There is a 10 s interval between steps. The displacement of each step is 0.5 cm, and the total compression of the sensor is 3.5 cm. The variation of voltage and force are synchronized in tests. The voltages do not change at the interval stages. However, the force relaxes right after each step due to the viscoelasticity of VHB layers [64,65].

Typically, teeth chew the food cyclically. We apply a symmetric triangle displacement profile to mimic chewing. To minimize the viscoelasticity and avoid negative compressive force in unloading process, we pre-compress the sensor by 2.5 cm, and wait for the full relaxation until there is no negative force when unloading. Then the sensor is tested under cyclic compression with amplitude of 1 cm and frequencies of (a) 0.8 Hz, (b) 1.2 Hz, and (c) 1.5 Hz (Fig. 5). The cyclic frequencies are selected according to the mean chewing frequency of human jaw [63,66]. The presented data spans 10 s in tests. The output voltage shows an instant response to the change of force. The linear relation between the force and voltage still stands for dynamic loading.

2.3. Improvements of materials and array design

To improve the biocompatibility of soft sensor, we replace acrylic elastomer by polydimethylsiloxane (PDMS) and ionic conductor by polyvinyl alcohol (PVA) hydrogel (Fig. 6a). PVA hydrogel is prepared through repetitive freeing-thawing process [67–69].

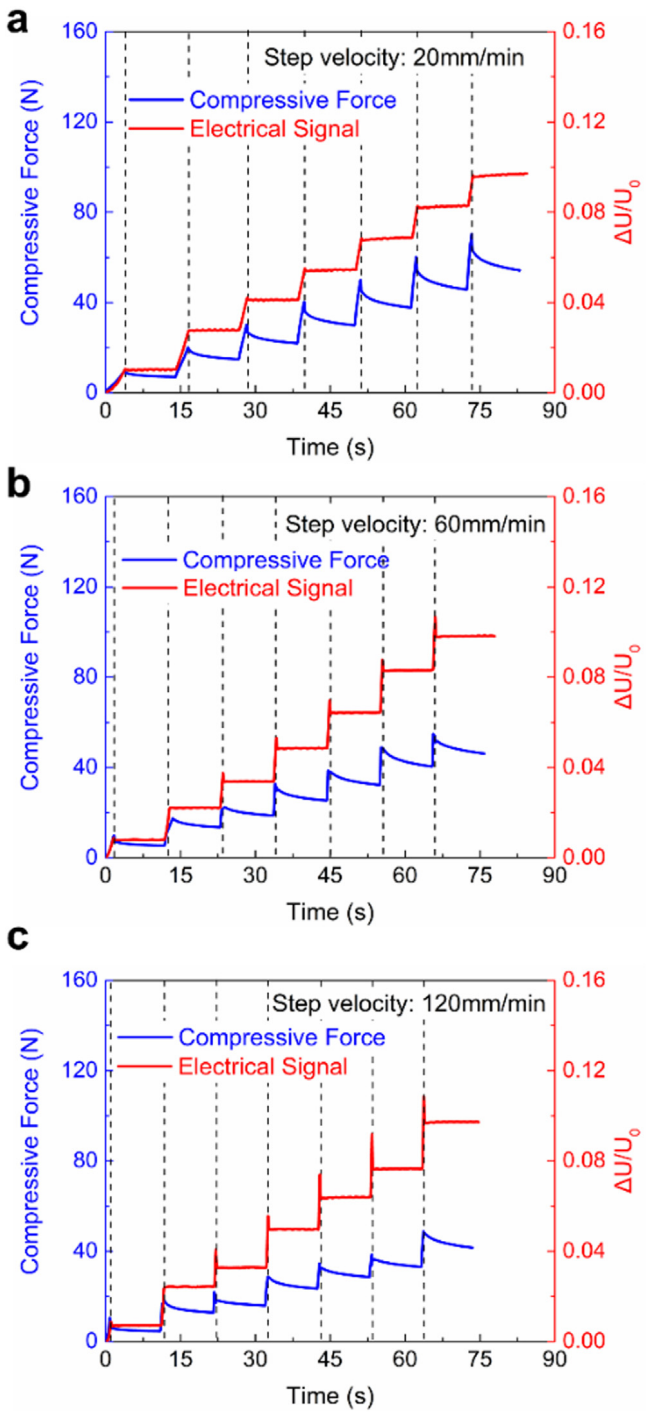

Fig. 4. The dynamic response of bite force sensor at different rates of step loading. The red curves represent the relative change of voltage, the blue curves represent the compressive force. The displacement of each step is 0.5 cm, the overall displacement of each test is 3.5 cm. The ramping rates in experiments are (a) 20 mm/min, (b) 60 mm/min, and (c) 120 mm/min. The voltages keep constant at the rest stage between steps. The forces show the relaxation in the intervals due to the viscoelasticity of dielectric elastomer.

Hydrogel with less PVA content shows lower modulus and larger stretchability (Figure S2). We use hydrogels consisting of 10 wt% PVA and physiological saline for sensors. The synthesis of PVA hydrogel and assembly of sensor are described in supporting information.

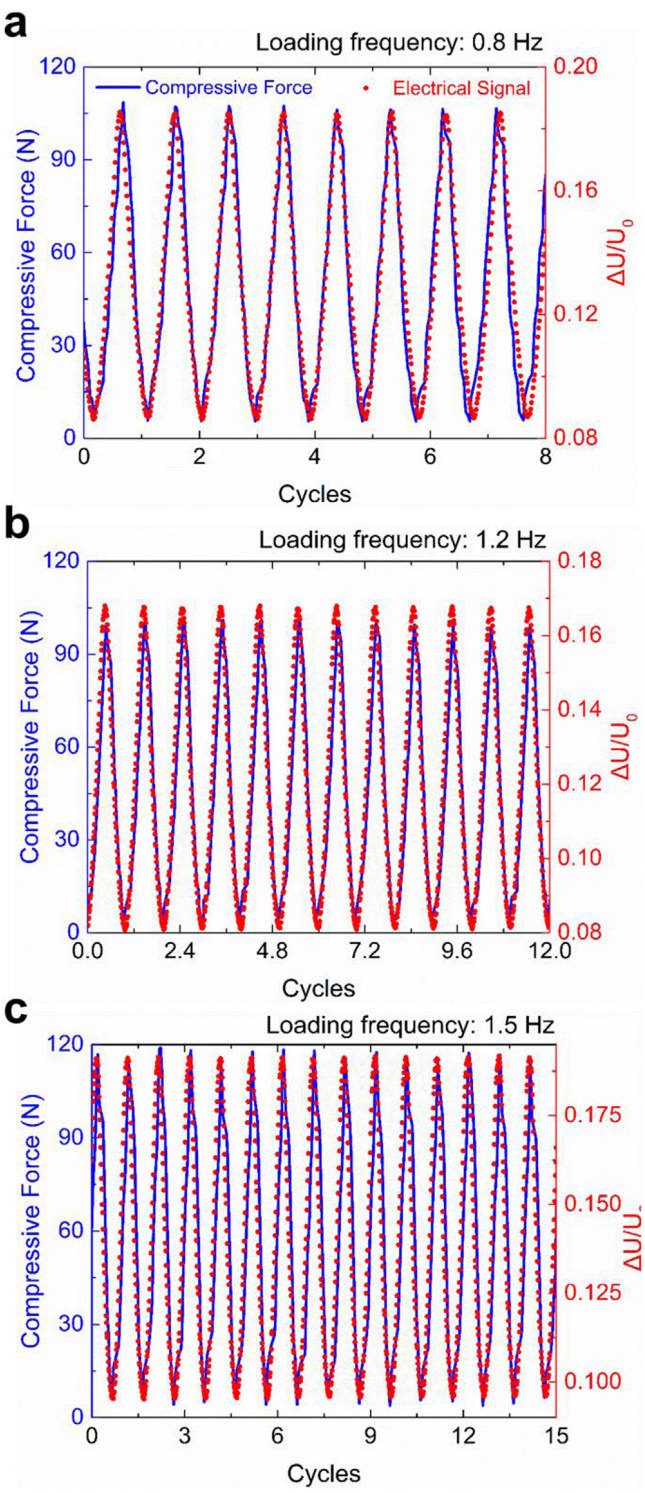

Fig. 5. The dynamic response of sensor under linear cyclic loading. The amplitude of compression is 1 cm. The frequencies are (a) 0.8 Hz, (b) 1.2 Hz, and (c) 1.5 Hz. The changes of voltage (red dots) and force (blue curves) are recorded simultaneously.

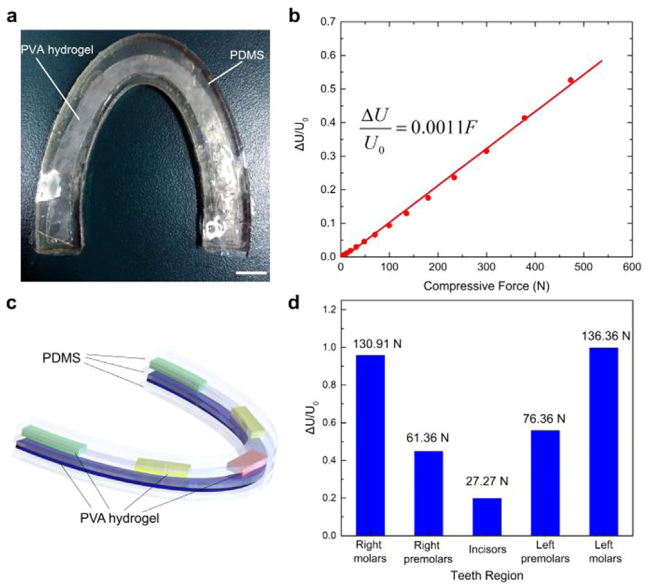

Fig. 6. Bite force sensor with biocompatible materials and array structure. (a) The photo of the sensor. The PVA hydrogels are opaque, and can be seen through the transparent PDMS layer. The scale bar is 10 mm. (b) Voltage variation is the linear function of full dentition bite force. Compressive force has reached the level of normal adult (∼500 N). (c) The soft sensor is designed with an array of ionic conductors on top and a line of ionic conductor on bottom. Green, yellow and red blocks indicate the sensing units for molars, premolars and incisors regions respectively. (d) Relative change of voltages in different dentition regions under the maximum load of 518 N. Blue bars show the relative variation of voltage before and after loading in each region. The corresponding forces are labelled above the bars . (For interpretation of the references to color in this figure legend, the reader is referred to the web version of this article.)

In addition, we reduce the thickness of hydrogel and insulating layer by half to increase the resolution of sensor. We test the full dentition sensor under quasi-static compression loading. Maximum displacement of the compression process is 2.5 cm. Force-voltage variation curve of full dentition bite force sensor is shown in linear relationship (Fig. 6b). The data can be linearly fitted as the $\Delta U/U_0 = 0.0011F$. We achieve the full dentition sensing with compression force around 50 kg, comparable to that of adults.

To measure the bite force in the different regions of dentition, we design an array of sensors for incisors, premolars, and molars (Fig. 6c). Gray layers are PDMS as insulating and encapsulating material. The blue layer represents a line of ionic conductor. Green, yellow and red blocks represent the array of ionic conductor located in molars, premolars and incisors regions. The area of each block accounts for 15% of the full dentition area. Afterwards, we test the sensor array under the full dentition compression (Fig. 6d). Relative variation of voltages is shown in different dentition regions under the maximum load of 518 N. The relative variation of voltage before and after loading in each region is labeled with corresponding force. According to the equation in Fig. 6b, the forces can be converted as $F_a = S_a \times \Delta U/U_0/0.0011$. Here $S_a$represents the areal ratio of sensor unit to full dentition bite region. Because each unit has same area, $S_a = 0.15$. Under full dentition test, molars bear more loads than premolars and incisors. This result is consistent with previous works [70,71]. Due to the less viscoelasticity of PDMS, stress relaxation during compression could be reduced and eventually the dynamic response of the biocompatible sensor could be better than that of original sensor.

3. Conclusion

In summary, we have demonstrated a soft bite force sensor using hydrogels and elastomers. The soft sensor readily conforms to the irregular surfaces of individual teeth, and captures bite forces from various regions of dentition simultaneously. It is hoped that the soft sensor will be further developed for applications in dental

care and research. It is also hoped that such soft sensors will be adapted to collect massive data for scientific studies of humans and other animals. This work illustrates the potential of using soft sensors to collect massive data over irregular and dynamic surfaces of hard materials. Other possible applications include machines and robots of hard materials.

Declaration of competing interest

The authors declare that they have no known competing financial interests or personal relationships that could have appeared to influence the work reported in this paper.

Acknowledgments

This work is supported by the National Natural Science Foundation of China (Grant Nos. 11172229 and 11321062). B. Chen and Z. Suo acknowledges the support of NSF MRSEC, PR China (DMR 14-20570).

References

[1] R.A. Anderson, L.D. McBrayer, A. Herrel, Bite force in vertebrates: opportunities and caveats for use of a nonpareil whole-animal performance measure, Biol. J. Linn. Soc. 93 (2008) 709–720.
[2] W.L. Korff, P.C. Wainwright, Motor pattern control for increasing crushing force in the striped burrfish (Chilomycterus schoepfi), Zoology 107 (2004) 335–346.
[3] A.K. Lappin, J.F. Husak, Weapon performance, not size, determines mating success and potential reproductive output in the collared lizard (Crotaphytus collaris), Am. Nat. 166 (2005) 426–436.
[4] S.E. Santana, E.R. Dumont, J.L. Davis, Mechanics of bite force production and its relationship to diet in bats, Funct. Ecol. 24 (2010) 776–784.
[5] D.R. Huber, J.M. Claes, J. Mallefet, A. Herrel, Is extreme bite performance associated with extreme morphologies in sharks?, Physiol. Biochem. Zool. 82 (2008) 20–28.
[6] A. Herrel, V. Holanova, Cranial morphology and bite force in Chamaeleolis lizards–adaptations to molluscivory?, Zoology 111 (2008) 467–475.
[7] A. Herrel, J. Podos, S. Huber, A. Hendry, Bite performance and morphology in a population of Darwin's finches: implications for the evolution of beak shape, Funct. Ecol. 19 (2005) 43–48.
[8] M.R. Nogueira, A.L. Peracchi, L.R. Monteiro, Morphological correlates of bite force and diet in the skull and mandible of phyllostomid bats, Funct. Ecol. 23 (2009) 715–723.
[9] S. Braun, H.-P. Bantleon, W.P. Hnat, J.W. Freudenthaler, M.R. Marcotte, B.E. Johnson, A study of bite force, part 1: Relationship to various physical characteristics, Angle Orthod. 65 (1995) 367–372.
[10] M. Bakke, Mandibular elevator muscles: physiology, action, and effect of dental occlusion, Eur. J. Oral. Sci. 101 (1993) 314–331.
[11] J. Ahlgren, B. Öwall, Muscular activity and chewing force: a polygraphic study of human mandibular movements, Arch. Oral. Biol. 15 (1970) 271–IN1.
[12] D. Lundgren, L. Laurell, Occlusal forces in prosthetically restored dentitions: a methodological study, J. Oral. Rehabil. 11 (1984) 29–37.
[13] K. Harada, M. Watanabe, K. Ohkura, S. Enomoto, Measure of bite force and occlusal contact area before and after bilateral sagittal split ramus osteotomy of the mandible using a new pressure-sensitive device: a preliminary report, J. Oral. Max. Surg. 58 (2000) 370–373.
[14] P.W. Freeman, C.A. Lemen, Measuring bite force in small mammals with a piezo-resistive sensor, J. Mammal. 89 (2008) 513–517.
[15] M. Iwase, M. Ohashi, H. Tachibana, T. Toyoshima, M. Nagumo, Bite force, occlusal contact area and masticatory efficiency before and after orthognathic surgical correction of mandibular prognathism, Int. J. Oral. Max. Surg. 35 (2006) 1102–1107.
[16] D. Koc, A. Dogan, B. Bek, Bite force and influential factors on bite force measurements: a literature review, Eur. J. Dent. 4 (2010) 223.
[17] A.D. Lantada, C.G. Bris, P.L. Morgado, J.S. Maudes, Novel system for bite-force sensing and monitoring based on magnetic near field communication, Sensors-Basel 12 (2012) 11544.
[18] A. Shimada, Y. Yamabe, T. Torisu, L. Baad-Hansen, H. Murata, P. Svensson, Measurement of dynamic bite force during mastication, J. Oral Rehabil. 39 (2012) 349–356.
[19] S. Umesh, S. Padma, S. Asokan, T. Srinivas, Fiber Bragg Grating based bite force measurement, J. Biomech. 49 (2016) 2877–2881.
[20] J. Fastier-Wooller, H.-P. Phan, T. Dinh, T.-K. Nguyen, A. Cameron, A. Öchsner, D. Dao, Novel low-cost sensor for human bite force measurement, Sensors 16 (2016) 1244.
[21] A. Diaz Lantada, C. González Bris, P. Lafont Morgado, J. Sanz Maudes, Novel system for bite-force sensing and monitoring based on magnetic near field communication, Sensors 12 (2012) 11544–11558.
[22] C. Serra, A. Manns, Bite force measurements with hard and soft bite surfaces, J. Oral. Rehabil. 40 (2013) 563–568.
[23] D.-H. Kim, N. Lu, R. Ma, R.-H. Kim Y.-.S, S. Wang, J. Wu, S.M. Won, H. Tao, A. Islam, Epidermal electronics, Science 333 (2011) 838–843.
[24] C. Keplinger, J.-Y. Sun, C.C. Foo, P. Rothemund, G.M. Whitesides, Z. Suo, Stretchable, transparent, ionic conductors, Science 341 (2013) 984–987.
[25] S. Park, H. Kim, M. Vosgueritchian, S. Cheon, H. Kim, J.H. Koo, T.R. Kim, S. Lee, G. Schwartz, H. Chang, Stretchable energy-harvesting tactile electronic skin capable of differentiating multiple mechanical stimuli modes, Adv. Mater. 26 (2014) 7324–7332.
[26] S. Xu, Y. Zhang, L. Jia, K.E. Mathewson, K.-I. Jang, J. Kim, H. Fu, X. Huang, P. Chava, R. Wang, Soft microfluidic assemblies of sensors, circuits, and radios for the skin, Science 344 (2014) 70–74.
[27] Y. Gao, J. Song, S. Li, C. Elowsky, Y. Zhou, S. Ducharme, Y.M. Chen, Q. Zhou, L. Tan, Hydrogel microphones for stealthy underwater listening, Nature Commun. 7 (2016) 12316.
[28] C.H. Yang, B. Chen, J. Zhou, Y.M. Chen, Z. Suo, Electroluminescence of giant stretchability, Adv. Mater. 28 (2016) 4480–4484.
[29] C.H. Yang, S. Zhou, S. Shian, D.R. Clarke, Z. Suo, Organic liquid-crystal devices based on ionic conductors, Mater. Horiz. 4 (2017) 1102–1109.
[30] S. Lin, H. Yuk, T. Zhang, G.A. Parada, H. Koo, C. Yu, X. Zhao, Stretchable hydrogel electronics and devices, Adv. Mater. 28 (2016) 4497–4505.
[31] M. Sasaki, B.C. Karikkineth, K. Nagamine, H. Kaji, K. Torimitsu, M. Nishizawa, Highly conductive stretchable and biocompatible electrode–hydrogel hybrids for advanced tissue engineering, Adv. Healthc. Mater. 3 (2014) 1919–1927.
[32] W. Zhang, J. Hu, J. Tang, Z. Wang, J. Wang, T. Lu, Z. Suo, Fracture toughness and fatigue threshold of tough hydrogels, ACS Macro Lett. 8 (2018) 17–23.
[33] R. Bai, B. Chen, J. Yang, Z. Suo, Tearing a hydrogel of complex rheology, J. Mech. Phys. Solids 125 (2019) 749–761.
[34] J.-Y. Sun, X. Zhao, W.R. Illeperuma, O. Chaudhuri, K.H. Oh, D.J. Mooney, J.J. Vlassak, Z. Suo, Highly stretchable and tough hydrogels, Nature 489 (2012) 133.
[35] J. Tang, J. Li, J.J. Vlassak, Z. Suo, Fatigue fracture of hydrogels, Extreme Mech. Lett. 10 (2017) 24–31.
[36] R. Bai, J. Yang, Z. Suo, Fatigue of hydrogels, Eur. J. Mech. A 74 (2019) 337–370.
[37] R. Bai, Q. Yang, J. Tang, X.P. Morelle, J. Vlassak, Z. Suo, Fatigue fracture of tough hydrogels, Extreme Mech. Lett. 15 (2017) 91–96.
[38] Q. Liu, G. Nian, C. Yang, S. Qu, Z. Suo, Bonding dissimilar polymer networks in various manufacturing processes, Nature Commun. 9 (2018) 846.
[39] J. Yang, R. Bai, B. Chen, Z. Suo, Hydrogel adhesion: A supramolecular synergy of chemistry, topology, and mechanics, Adv. Funct. Mater. (2019) 1901693.
[40] Y. Gao, K. Wu, Z. Suo, Photodetachable adhesion, Adv. Mater. (2018) 1806948.
[41] B. Chen, J.J. Lu, C.H. Yang, J.H. Yang, J. Zhou, Y.M. Chen, Z. Suo, Highly stretchable and transparent ionogels as nonvolatile conductors for dielectric elastomer transducers, ACS Appl. Mater. Interfaces 6 (2014) 7840–7845.
[42] J. Li, Z. Suo, J.J. Vlassak, Stiff, strong, and tough hydrogels with good chemical stability, J. Mater. Chem. B 2 (2014) 6708–6713.
[43] P. Le Floch, X. Yao, Q. Liu, Z. Wang, G. Nian, Y. Sun, L. Jia, Z. Suo, Wearable and washable conductors for active textiles, ACS Appl. Mater. Interfaces 9 (2017) 25542–25552.
[44] N. Rauner, M. Meuris, M. Zoric, J.C. Tiller, Enzymatic mineralization generates ultrastiff and tough hydrogels with tunable mechanics, Nature 543 (2017) 407.
[45] K. Tian, J. Bae, S.E. Bakarich, C. Yang, R.D. Gately, G.M. Spinks, M. in het Panhuis, Z. Suo, J.J. Vlassak, 3D Printing of transparent and conductive heterogeneous hydrogel–elastomer systems, Adv. Mater. 29 (2017) 160482.
[46] W. Hong, X. Zhao, J. Zhou, Z. Suo, A theory of coupled diffusion and large deformation in polymeric gels, J. Mech. Phys. Solids 56 (2008) 1779–1793.
[47] Z. Suo, Theory of dielectric elastomers, Acta Mech. Solida Sin. 23 (2010) 549–578.
[48] T. Lu, J. Huang, C. Jordi, G. Kovacs, R. Huang, D.R. Clarke, Z. Suo, Dielectric elastomer actuators under equal-biaxial forces, uniaxial forces, and uniaxial constraint of stiff fibers, Soft Matter 8 (2012) 6167–6173.
[49] Z. Suo, Mechanics of stretchable electronics and soft machines, MRS Bull. 37 (2012) 218–225.
[50] L. An, F. Wang, S. Cheng, T. Lu, T. Wang, Experimental investigation of the electromechanical phase transition in a dielectric elastomer tube, Smart Mater. Struct. 24 (2015) 035006.
[51] T. Lu, S. Cheng, T. Li, T. Wang, Z. Suo, Electromechanical catastrophe, Int. J. Appl. Mech. 8 (2016) 1640005.

[52] J. Tang, J. Li, J.J. Vlassak, Z. Suo, Adhesion between highly stretchable materials, Soft Matter 12 (2016) 1093–1099.
[53] C. Chen, Z. Wang, Z. Suo, Flaw sensitivity of highly stretchable materials, Extreme Mech. Lett. 10 (2017) 50–57.
[54] T. Lu, Z. Shi, Q. Shi, T. Wang, Bioinspired bicipital muscle with fiber-constrained dielectric elastomer actuator, Extreme Mech. Lett. 6 (2016) 75–81.
[55] T. Li, G. Li, Y. Liang, T. Cheng, J. Dai, X. Yang, B. Liu, Z. Zeng, Z. Huang, Y. Luo, Fast-moving soft electronic fish, Sci. Adv. 3 (2017) e1602045.
[56] B. Chen, Y. Bai, F. Xiang, J.Y. Sun, Y. Mei Chen, H. Wang, J. Zhou, Z. Suo, Stretchable and transparent hydrogels as soft conductors for dielectric elastomer actuators, J. Polym. Sci. B 52 (2014) 1055–1060.
[57] C.H. Yang, B. Chen, J.J. Lu, .H. Yang, J. Zhou, Y.M. Chen, Z. Suo, Ionic cable, Extreme Mech. Lett. 3 (2015) 59–65.
[58] J.Y. Sun, C. Keplinger, G.M. Whitesides, Z. Suo, Ionic skin, Adv. Mater. 26 (2014) 7608–7614.
[59] C.-C. Kim, H.-H. Lee, K.H. Oh, J.-Y. Sun, Highly stretchable, transparent ionic touch panel, Science 353 (2016) 682–687.
[60] M.S. Sarwar, Y. Dobashi, C. Preston, J.K. Wyss, S. Mirabbasi, J.D.W. Madden, Bend, stretch, and touch: Locating a finger on an actively deformed transparent sensor array, Sci. Adv. 3 (2017) e1602200.
[61] S. Cheng, Y.S. Narang, C. Yang, Z. Suo, R.D. Howe, Stick-on large-strain sensors for soft robots, Adv. Mater. Interfaces (2019) in press. Published online.
[62] C.H. Yang, M.X. Wang, H. Haider, J.H. Yang, J.-Y. Sun, Y.M. Chen, J. Zhou, Z. Suo, Strengthening alginate/polyacrylamide hydrogels using various multivalent cations, ACS Appl. Mater. Interfaces 5 (2013) 10418–10422.
[63] B. Bishop, O. Plesh, W. McCall Jr., Effects of chewing frequency and bolus hardness on human incisor trajectory and masseter muscle activity, Arch. Oral. Biol. 35 (1990) 311–318.
[64] M. Hossain, D.K. Vu, P. Steinmann, Experimental study and numerical modelling of VHB 4910, polymer, Comput. Mater. Sci. 59 (2012) 65–74.
[65] M. Kollosche, G. Kofod, Z. Suo, J. Zhu, Temporal evolution and instability in a viscoelastic dielectric elastomer, J. Mech. Phys. Solids 76 (2015) 47–64.
[66] M. Farella, M. Bakke, A. Michelotti, R. Martina, Effects of prolonged gum chewing on pain and fatigue in human jaw muscles, Eur. J. Oral. Sci. 109 (2001) 81–85.
[67] M.I. Baker, S.P. Walsh, Z. Schwartz, B.D. Boyan, A review of polyvinyl alcohol and its uses in cartilage and orthopedic applications, J. Biomed. Mater. Res. B 100 (2012) 1451–1457.
[68] T.H. Elshazly, Characterization of PVA Hydrogels with Regards To Vascular Graft Development, Georgia Institute of Technology, 2004.
[69] J.A. Stammen, S. Williams, D.N. Ku, R.E. Guldberg, Mechanical properties of a novel PVA hydrogel in shear and unconfined compression, Biomaterials 22 (2001) 799–806.
[70] S.C.H. Regalo, C.M. Santos, M. Vitti, C.A. Regalo, P.B. de Vasconcelos, W. Mestriner Jr., M. Semprini, F.J. Dias, J.E.C. Hallak, S. Siéssere, Evaluation of molar and incisor bite force in indigenous compared with white population in Brazil, Arch. Oral. Biol. 53 (2008) 282–286.
[71] G.S. Tate, E. Ellis III, G. Throckmorton, Bite forces in patients treated for mandibular angle fractures: implications for fixation recommendations, J. Oral. Max. Surg. 52 (1994) 734–736.